Mineralogical Magazine, August 2017, Vol. 81(4), pp. 909–916

Chinleite-(Y), $NaY(SO_4)_2 \cdot H_2O$, a new rare-earth sulfate mineral structurally related to bassanite

ANTHONY R. KAMPF[1,*], BARBARA P. NASH[2] AND JOE MARTY[3]

[1] Mineral Sciences Department, Natural History Museum of Los Angeles County, 900 Exposition Boulevard, Los Angeles, CA 90007, USA
[2] Department of Geology and Geophysics, University of Utah, Salt Lake City, Utah 84112, USA
[3] 5199 East Silver Oak Road, Salt Lake City, UT 84108, USA

[*Received 23 June 2016; Accepted 28 July 2016; Associate Editor: Andrew Christy*]

ABSTRACT

The new mineral chinleite-(Y) (IMA2016-017), $NaY(SO_4)_2 \cdot H_2O$, was found in the Blue Lizard mine, San Juan County, Utah, USA, where it occurs as a secondary alteration phase. Chinleite-(Y) crystals are thin hexagonal {100} prisms (up to 0.3 mm long) with pyramidal terminations consisting of the forms {101} and {011}. Prisms are typically intergrown in divergent sprays, bow-tie aggregates or subparallel intergrowths. Crystals are colourless and transparent with a vitreous lustre. The streak is white and the mineral is nonfluorescent. The Mohs hardness is between 2½ and 3. Crystals are brittle with at least one good cleavage parallel to [001], probably {100}, and have splintery fracture. The mineral is slowly soluble in H_2O at room temperature. The calculated density is 3.385 g cm^{-3}. The mineral is optically uniaxial (+), with $\omega = 1.565(1)$ and $\varepsilon = 1.603(1)$ (white light). Electron microprobe analyses yielded the empirical formula $(Na_{0.507}Ca_{0.285}Y_{0.176})_{\Sigma 0.968}(Y_{0.724}Dy_{0.110}Er_{0.053}Gd_{0.037}Ho_{0.021}Yb_{0.013}Nd_{0.014}Eu_{0.005}Sm_{0.008}Ce_{0.010}Pr_{0.003}La_{0.002})_{\Sigma 1.000}(SO_4)_2 \cdot H_{1.401}O$. The eight strongest powder X-ray diffraction lines are [d_{obs} Å (I)(hkl)]: 6.01(59)(100), 5.43(63)(011), 3.457(46)(110), 3.010(100)(200), 2.826(95)(014), 2.1365(39) (006,122), 1.8493(67)(214) and 1.6901(28)(125,034). Chinleite-(Y) is trigonal, $P3_221$, $a = 6.890(2)$, $c = 12.767(2)$ Å, $V = 524.9(3)$ Å^3 and $Z = 3$. The structure of chinleite-(Y) ($R_1 = 0.0444$ for 303 $F_o > 4\sigma F$), a three-dimensional framework, consisting of SO_4 groups, irregular NaO_8 polyhedra and YO_9 distorted tri-capped trigonal prisms, is similar to the structure of bassanite.

KEYWORDS: chinleite-(Y), new mineral, rare-earth sulfate, crystal structure, bassanite, Blue Lizard mine, Utah, USA.

Introduction

CHINLEITE-(Y) is the fifteenth new mineral to be first described from the Blue Lizard uranium mine in southeast Utah (see table 1 in Kampf *et al.*, 2017*a*). This mine has quickly become the world's most prolific source of new uranyl sulfate minerals, with 12 described so far, compared with the closest competitor, the Svornost mine at Jáchymov, Czech Republic, with a total of six. Chinleite-(Y) is the third sulfate mineral not containing uranyl that has been described from the Blue Lizard mine. The only other rare-earth mineral found so far at the mine is the recently described uranyl sulfate, alwilkinsite-(Y), $Y(H_2O)_7[(UO_2)_3(SO_4)_2O(OH)_3] \cdot 7H_2O$ (Kampf *et al.*, 2017*a*).

Chinleite (/'tSin lei ait/) is named for the Chinle Formation of Upper Triassic age, in which the deposit exploited by the Blue Lizard mine occurs. The word 'chinle' means 'flowing out' in the Navajo language, and is a reference to the location where the water flows out of the Canyon de Chelly in Arizona. The '-(Y)' suffix is the Levinson modifier indicating the dominance of Y over other rare earth elements in the mineral. The new mineral and name were approved by the Commission on

---

*E-mail: akampf@nhm.org
https://doi.org/10.1180/minmag.2016.080.140

TABLE 1. Chemical composition (in wt.%) for chinleite-(Y).

Constituent	Mean	Range	Stand. dev.	Probe standard
Na_2O	4.36	3.50–5.28	0.63	albite
CaO	4.44	3.31–5.57	0.87	diopside
Y_2O_3	28.17	23.68–31.56	3.01	YAG
La_2O_3	0.10	0.00–0.27	0.12	LaF_3
Ce_2O_3	0.44	0.15–0.82	0.27	CeF_3
Pr_2O_3	0.12	0.00–0.45	0.17	PrF_3
Nd_2O_3	0.64	0.14–1.32	0.46	NdF_3
Sm_2O_3	0.40	0.02–0.95	0.37	Sm metal
Eu_2O_3	0.24	0.00–0.52	0.21	EuF_3
Gd_2O_3	1.84	0.72–3.76	1.07	Gd metal
Dy_2O_3	5.67	4.79–7.22	0.86	Dy metal
Ho_2O_3	1.10	0.93–1.26	0.10	Ho metal
Er_2O_3	2.79	2.39–3.36	0.33	Er metal
Yb_2O_3	0.73	0.00–1.07	0.40	Yb metal
SO_3	44.41	40.18–47.32	2.20	celestine
H_2O*	3.50			
Total	98.95			

*Based on the structure (O = 9 atoms per formula unit).

New Minerals, Nomenclature and Classification of the International Mineralogical Association (IMA2016-017). The description is based on three cotype specimens deposited in the collections of the Natural History Museum of Los Angeles County, 900 Exposition Boulevard, Los Angeles, CA 90007, USA, catalogue numbers 65632, 65633 and 65634.

Occurrence

Chinleite-(Y) was found underground in the Blue Lizard mine, Red Canyon, White Canyon district, San Juan County, Utah, USA (37°33′26″N 110°17′44″W). The Blue Lizard mine is located ~72 km west of the town of Blanding, Utah, and ~22 km southeast of Good Hope Bay on Lake Powell. Information on the history and geology of the deposit is taken largely from Chenoweth (1993).

Mineralized channels are in the Shinarump member of the Chinle Formation. The Shinarump member consists of medium- to coarse-grained sandstone, conglomeratic sandstone beds and thick siltstone lenses. Ore minerals were deposited as replacements of wood and other organic material and as disseminations in the enclosing sandstone. Since the mine closed in 1978, oxidation of primary ores in the humid underground environment has produced a variety of secondary minerals, mainly sulfates, as efflorescent crusts on the surfaces of mine walls.

Chinleite-(Y) is a rare mineral, so far having been found on only a few specimens. The other secondary minerals found in direct association with chinleite-(Y) are gypsum, hexahydrite, johannite, metauranospinite, natrojarosite and other potentially new minerals. The bulk of the matrix is comprised of subhedral to euhedral, equant quartz crystals that are recrystallized counterparts of the original grains of the sandstone. Other minerals remaining from the original sandstone include feldspar and rare detrital almandine and zircon. An exhaustive list of other secondary minerals found in our studies of the Blue Lizard secondary assemblages can be found in Kampf *et al.* (2017*b*).

Chinleite-(Y) and the other minerals in the secondary assemblages in the Blue Lizard mine formed at ambient temperature by evaporative processes at the surface of a rock with high relative porosity. The environment is relatively oxidizing (high Eh) and solutions are generally acidic (low pH). The low molar proportion of H_2O in chinleite-(Y) suggests that it formed at moderately low relative humidity. A detailed discussion of the origin and conditions of formation of the uranyl sulfate assemblages at the Blue Lizard mine was provided by Plášil *et al.* (2014) and was more recently summarized by Kampf *et al.* (2017*b*). As noted by Kampf *et al.* (2017*a*), the Y, as well as other rare-earth elements (*REE*s) found in lesser amounts, in chinleite-(Y) and alwilkinsite-(Y) probably existed in the sandstones of the Chinle Formation prior to the deposition of the U ores.

Physical and optical properties

Chinleite-(Y) crystals are thin hexagonal {100} prisms with pyramidal terminations consisting of the forms {101} and {011} (Fig. 1). Prisms are up to ~0.3 mm long and are typically intergrown in divergent sprays, bow-tie aggregates or subparallel intergrowths (Fig. 2). Merohedral twinning is indicated by the structure refinement. Crystals are colourless and transparent with a vitreous lustre. The streak is white. The mineral is nonfluorescent. The Mohs hardness is estimated to be between 2½ and 3, based upon the behaviour of crystals when broken. Crystals are brittle with at least one good cleavage parallel to [001], probably {100}, and have splintery fracture. The mineral is slowly soluble in H_2O at room temperature. The density could not be measured because the mineral is soluble in Clerici solution. The calculated density is 3.385 g cm^{-3} based on the empirical formula.

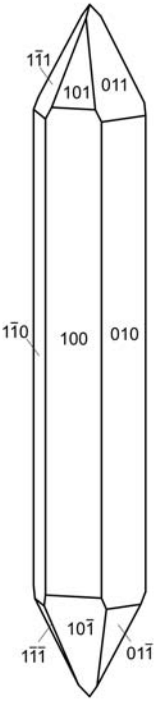

FIG. 1. Crystal drawing of chinleite-(Y), clinographic projection in standard orientation.

FIG. 2. Chinleite-(Y) with natrojarosite (yellow) on quartz; field of view: 0.5 mm across.

Optically, chinleite-(Y) is uniaxial (+), with ω = 1.565(1) and ε = 1.603(1), measured in white light. No pleochroism was observed.

Composition

Chemical analyses (7 points on 3 crystals) were performed at the University of Utah on a Cameca SX-50 electron microprobe with four wavelength dispersive spectrometers using *Probe for EPMA* software. Analytical conditions were 15 kV accelerating voltage, 20 nA beam current and a beam diameter of 5 µm. Counting times were 30 s on peak and 30 s on background for Ca and S and 20/20 for all other elements. Time-dependent intensity corrections were applied to Na, S and *REE*s (including Y). Raw X-ray intensities were corrected for matrix effects with a ϕρ(z) algorithm (Pouchou and Pichoir, 1991). No damage from the electron beam was observed. Because insufficient material was available for a direct determination of H_2O, it has been calculated based upon the structure determination. Analytical data are given in Table 1.

The empirical formula (based on 2 S and 9 O atoms per formula unit) is $(Y_{0.900}Na_{0.507}Ca_{0.285}Dy_{0.110}Er_{0.053}Gd_{0.037}Ho_{0.021}Yb_{0.013}Nd_{0.014}Eu_{0.005}Sm_{0.008}Ce_{0.010}Pr_{0.003}La_{0.002})_{\Sigma 1.968}S_2O_9H_{1.401}$, or with cations assigned to structural sites, $(Na_{0.507}Ca_{0.285}Y_{0.176})_{\Sigma 0.968}(Y_{0.724}Dy_{0.110}Er_{0.053}Gd_{0.037}Ho_{0.021}Yb_{0.013}Nd_{0.014}Eu_{0.005}Sm_{0.008}Ce_{0.010}Pr_{0.003}$

TABLE 2. Powder X-ray data (d in Å) for chinleite-(Y). Only calculated lines with intensities >4 are included.

I_{obs}	d_{obs}	d_{calc}	I_{calc}	$h\ k\ l$
59	6.01	5.9669	83	1 0 0
63	5.43	5.4057	86	0 1 1
		4.3591	6	1 0 2
15	4.315	4.2557	14	0 0 3
46	3.457	3.4450	59	1 1 0
6	3.352	3.3260	9	1 1 1
100	3.010	2.9835	88	2 0 0
		2.9052	5	2 0 1
95	2.826	2.8144	100	0 1 4
		2.6776	5	1 1 3
7	2.452	2.4429	11	0 2 3
14	2.347	2.3475	8	1 0 5
		2.3413	13	1 1 4
13	2.231	2.2553	8	2 1 0
		2.2209	11	2 1 1
		2.1795	6	0 2 4
39	2.1365	2.1278	11	0 0 6
		2.1265	27	1 2 2
4	2.0409	2.0514	5	1 1 5
8	1.9784	1.9927	4	2 1 3
		1.9653	7	0 3 1
13	1.8995	1.8989	10	3 0 2
67	1.8493	1.8419	58	2 1 4
14	1.7308	1.7324	5	0 2 6
		1.7225	6	2 2 0
28	1.6901	1.6903	6	1 2 5
		1.6880	22	0 3 4
10	1.6549	1.6549	17	3 1 0

TABLE 3. Data collection and structure refinement details for chinleite-(Y).*

Diffractometer	Rigaku R-Axis Rapid II
X-ray radiation/power	Mo$K\alpha$ ($\lambda = 0.71075$Å)/50 kV, 40 mA
Temperature	298(2) K
Structural Formula	$(Na_{0.91}Y_{0.09})(Y_{0.72}Dy_{0.28})(SO_4)_2{\cdot}H_2O$
Space group	$P3_221$
Unit-cell dimensions	$a = 6.890(2)$ Å $c = 12.767(2)$ Å
V	524.9(3) Å^3
Z	3
Density (for above formula)	3.316 g cm^{-3}
Absorption coefficient	10.444 mm^{-1}
F(000)	499
Crystal size (μm)	35 × 30 × 20
θ range	3.41 to 20.00°
Index ranges	$-6 \leq h \leq 6$, $-6 \leq k \leq 6$, $-10 \leq l \leq 12$
Reflections collected/unique	1572/334; $R_{int} = 0.057$
Reflections with $F_o > 4\sigma(F)$	303
Completeness to $\theta = 20.00°$	100%
Refinement method	Full-matrix least-squares on F^2
Restraints/parameters	0/63
Goof	1.204
Final R indices [$F > 4\sigma(F)$]	$R_1 = 0.0444$, $wR_2 = 0.1027$
R indices (all data)	$R_1 = 0.0506$, $wR_2 = 0.1074$
Flack parameter	0.13(8)
Extinction coefficient	0.007(3)
Largest diff. peak/hole	+0.79/–0.91 e A^{-3}

*$R_{int} = \Sigma|F_o^2 - F_o^2(\text{mean})|/\Sigma[F_o^2]$. Goof $= S = \{\Sigma[w(F_o^2 - F_c^2)^2]/(n-p)\}^{1/2}$. $R_1 = \Sigma||F_o| - |F_c||/\Sigma|F_o|$. $wR_2 = \{\Sigma[w(F_o^2 - F_c^2)^2]/\Sigma[w(F_o^2)^2]\}^{1/2}$; $w = 1/[\sigma^2(F_o^2) + (aP)^2 + bP]$ where a is 0.042, b is 6.0316 and P is $[2F_c^2 + \text{Max}(F_o^2,0)]/3$.

TABLE 4. Atom coordinates and displacement parameters (Å^2) for chinleite-(Y).

	x/a	y/b	z/c	$U_{\mathrm{eq/iso}}$		
Na*	0.4672(16)	0	0.1667	0.027(5)		
Y*	0.5620(5)	0.5620(5)	0	0.0236(13)		
S	0.4538(11)	0.0093(12)	0.9102(4)	0.018(2)		
O1	0.502(4)	0.879(4)	0.9832(11)	0.035(5)		
O2	0.485(3)	0.357(3)	0.1714(9)	0.027(5)		
O3	0.741(2)	0.614(3)	0.8233(11)	0.034(5)		
O4	0.167(3)	0.416(3)	0.0275(13)	0.031(5)		
O5	0.910(5)	0.910(5)	0	0.055(11)§		
	U^{11}	U^{22}	U^{33}	U^{23}	U^{13}	U^{12}
Na*	0.036(7)	0.015(8)	0.024(7)	0.003(6)	0.001(3)	0.007(4)
Y*	0.0285(16)	0.0285(16)	0.0176(17)	−0.0003(8)	0.0003(8)	0.0171(19)
S	0.022(4)	0.020(4)	0.013(3)	0.002(3)	0.002(3)	0.012(3)
O1	0.039(15)	0.046(13)	0.015(9)	−0.005(10)	−0.006(9)	0.019(11)
O2	0.055(16)	0.034(10)	0.011(9)	−0.002(7)	0.000(10)	0.037(12)
O3	0.031(12)	0.048(14)	0.019(8)	−0.002(9)	−0.016(9)	0.018(11)
O4	0.039(11)	0.030(11)	0.022(9)	−0.009(8)	0.006(8)	0.017(10)

*Refined occupancies: Y site: Y/Dy = 0.72/0.28(3); Na site: Na/Y = 0.908/0.092(19).

$^{\S}U_{\mathrm{iso}}$.

$\mathrm{La_{0.002})_{\Sigma 1.000}(SO_4)_2 \cdot H_{1.401}O}$. (Note that 1.401 rather than 2 H is assigned for charge balance.) The simplified end-member formula is $\mathrm{NaY(SO_4)_2 \cdot H_2O}$, which requires $\mathrm{Na_2O}$ 9.62, $\mathrm{Y_2O_3}$ 35.06, $\mathrm{SO_3}$ 49.72 and $\mathrm{H_2O}$ 5.59, total 100 wt.%.

The Gladstone-Dale compatibility index $1 - (K_P/K_C)$ for the empirical formula is –0.021, in the excellent range (Mandarino, 2007).

X-ray crystallography and structure refinement

Powder X-ray studies were carried out using a Rigaku R-Axis Rapid II curved imaging plate microdiffractometer, with monochromatized Mo$K\alpha$ radiation ($\lambda = 0.71075$ Å). A Gandolfi-like motion on the φ and ω axes was used to randomize the sample and observed d-values and intensities were derived by profile fitting using *JADE 2010* software (Materials Data, Inc.). The powder data presented in Table 2 show good agreement with the pattern calculated from the structure determination. Unit-cell parameters refined from the powder data using *JADE 2010* with whole pattern fitting are: $a = 6.9118(16)$, $c = 12.792(3)$ Å and $V = 529.2(3)$ Å^3.

The single-crystal structure data for chinleite-(Y) were collected at room temperature on the same instrument and with the same radiation noted above. The data were processed using the Rigaku *CrystalClear* software package and an empirical (multi-scan) absorption correction was applied using the *ABSCOR* program (Higashi, 2001) in the *CrystalClear* software suite. The structure was solved by direct methods using *SIR2011* (Burla *et al.*, 2012). *SHELXL-2013* (Sheldrick, 2008) was used for the refinement of the structure. The small

TABLE 5. Selected bond distances (Å) for chinleite-(Y).

Na–O2(×2)	2.401(17)	Y–O5	2.40(4)	S–O1	1.44(2)	Hydrogen bonds	
Na–O3(×2)	2.454(19)	Y–O4(×2)	2.409(16)	S–O2	1.466(16)	O5–O3	3.233(19)
Na–O1(×2)	2.539(15)	Y–O1(×2)	2.42(2)	S–O3	1.469(15)	O5–O4	3.04(4)
Na–O4(×2)	2.828(17)	Y–O3(×2)	2.510(15)	S–O4	1.471(16)		
<Na–O>	2.556	Y–O2(×2)	2.513(13)	<S–O>	1.462		
		<Y–O>	2.456				

TABLE 6. Bond-valence analysis for chinleite-(Y). Values are expressed in valence units.

	O1	O2	O3	O4	O5	Σ
Na	0.11	0.16	0.14	0.05		0.92
Y	0.33	0.25	0.25	0.34	0.35	2.69
S1	1.64	1.53	1.52	1.51		6.21
H			0.10		0.90	1.00
H				0.12	0.88	1.00
Σ	2.08	1.94	2.01	2.02	2.13	

Bond valences are based on full occupancies of the Na and Y sites by Na and Y, respectively. Na^+–O bond-valence parameters from Wood and Palenik (1999); Y^{3+}–O from Krivovichev (2012); S^{6+}–O from Brown and Altermatt (1985); hydrogen-bond strengths based on O–O bond lengths from Ferraris and Ivaldi (1988).

size of the crystal fragment limited the data to a maximum θ of 20°; however, the data was of sufficient quality to refine all sites with anisotropic displacement parameters, except for the O5 site corresponding to the H_2O group. The Y site was refined with joint occupancy by Y and Dy, yielding a site-scattering value of 139.68. Assigning the Y site full occupancy by the constituents indicated by the empirical formula, $(Y_{0.724}Dy_{0.110}Er_{0.053}Gd_{0.037}Ho_{0.021}Yb_{0.013}Nd_{0.014}Eu_{0.005}Sm_{0.008}Ce_{0.010}Pr_{0.003}La_{0.002})_{\Sigma 1.000}$, yields a site-scattering value of 138.73, in close agreement with the aforementioned refined value. The Na site was refined with joint occupancy by Na and Y, yielding a site-scattering value of 40.73. This is significantly lower than the site-scattering value of 54.42 based on the site occupancy indicated by the empirical formula, $(Na_{0.507}Ca_{0.285}Y_{0.176})_{\Sigma 0.968}$. The most likely explanation is that the crystal used for the structure determination was higher in Na and/or Ca and lower in Y than the mean results from electron probe microanalysis (EPMA). The large variations in these elements noted during the EPMA further support this explanation. Data collection and refinement details are given in

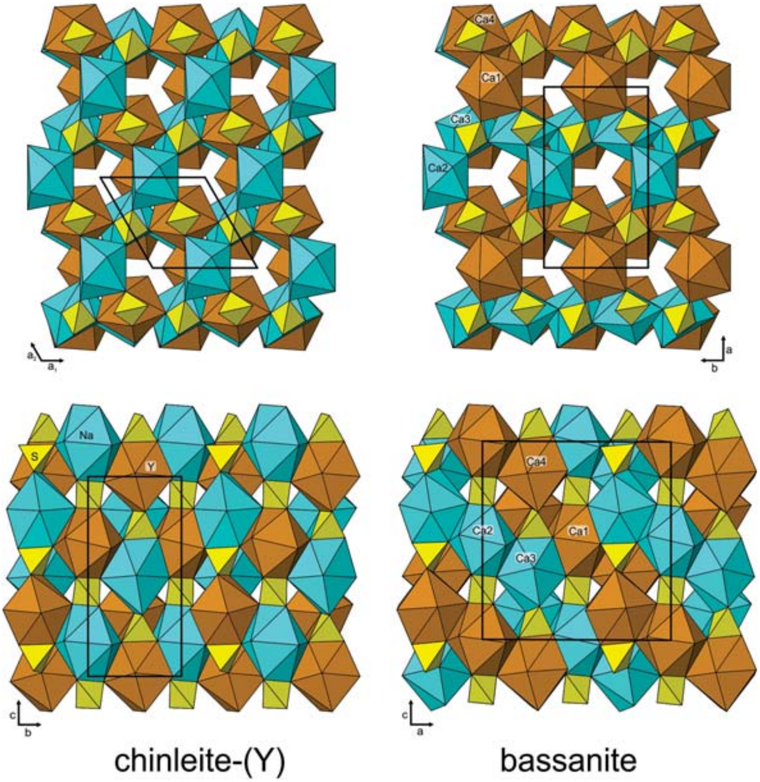

FIG. 3. The structures of chinleite-(Y) and bassanite. 8-coordinated polyhedra are blue and 9-coordinated polyhedra are orange. Unit-cell outlines are shown as thick black lines.

Table 3, atom coordinates and displacement parameters in Table 4, selected bond distances in Table 5 and a bond valence analysis in Table 6.

Discussion of the structure

Chinleite-(Y) is isostructural with the synthetic Na-*REE* ternary sulfate monohydrates, Na*REE*$(SO_4)_2 \cdot H_2O$ (cf. Perles *et al.*, 2005). The structure of chinleite-(Y) (Fig. 3) is a three-dimensional framework, consisting of SO_4 groups, irregular NaO_8 polyhedra and YO_9 distorted tri-capped trigonal prisms. The eight O atoms coordinated to Na^+ are from six SO_4 groups. The Y^{3+} is coordinated to the O atom (O5) from the H_2O group and to eight O atoms from six SO_4 groups. Each of the four O atoms (O1, O2, O3 and O4) of the SO_4 group bonds to one Na and one Y. The O3 and O4 atoms also accept hydrogen bonds from the H_2O group, consistent with the S–O3 and S–O4 bonds, 1.469 and 1.470 Å, being the longest in the SO_4 group. On the other hand, there is no obvious topological or geometrical explanation for the shortness of the 1.44(2) Å S–O1 bond, compared with the 1.466 Å S–O2 bond.

A distinctive feature of the chinleite-(Y) structure is an edge-sharing chain along [001] in which two opposite edges of the SO_4 group share edges with NaO_8 and YO_9 polyhedra. This same type of chain is also found in the structures of bassanite, $Ca(SO_4)(H_2O)_{0.5}$ (Ballirano *et al.*, 2001) and the members of the rhabdophane group (cf. Atkin *et al.*, 1983). In all of these structures, adjacent chains are joined to one another by sharing edges of the 8- and/or 9-coordinated polyhedra, each of which shares four nonadjacent edges with other 8- and/or 9-coordinated polyhedra.

The structure of chinleite-(Y) is particularly similar to that of bassanite (Fig. 3), in which Ca is both 8 and 9 coordinated. The structures differ, however, in the linkages of these polyhedra. In the structure of chinleite-(Y), NaO_8 polyhedra share edges only with YO_9 polyhedra and vice versa, while in the bassanite structure, the $Ca1O_9$ polyhedron shares edges with two different $Ca4O_9$ polyhedra, the $Ca2O_8$ polyhedron shares edges with two different $Ca3O_8$ polyhedra, the $Ca3O_8$ polyhedron shares an edge with a $Ca2O_8$ polyhedra and an edge with a $Ca1O_9$ polyhedron, and the $Ca4O_9$ polyhedron shares an edge with a $Ca1O_9$ polyhedra and an edge with a $Ca2O_8$ polyhedron. In the structures of both chinleite-(Y) and bassanite, one vertex of the 9-coordinated polyhedra is an H_2O group and is unshared with any other polyhedra. In contrast, the rhabdophane structure has only one type of large polyhedron, which is 8-coordinated.

Acknowledgements

Two anonymous reviewers are thanked for their constructive comments on the manuscript. A portion of this study was funded by the John Jago Trelawney Endowment to the Mineral Sciences Department of the Natural History Museum of Los Angeles County.

References

Atkin, D., Basham, I.R. and Bowles, J.F.W. (1983) Tristramite, a new calcium uranium phosphate of the rhabdophane group. *Mineralogical Magazine*, **47**, 393–396.

Ballirano, P., Maras, A., Meloni, S. and Caminiti, R. (2001) The monoclinic *I*2 structure of bassanite, calcium sulphate hemihydrate. *European Journal of Mineralogy*, **13**, 985–993.

Brown, I.D. and Altermatt, D. (1985) Bond-valence parameters from a systematic analysis of the inorganic crystal structure database. *Acta Crystallographica*, **B41**, 244–247.

Burla, M.C., Caliandro, R., Camalli, M., Carrozzini, B., Cascarano, G.L., Giacovazzo, C., Mallamo, M., Mazzone, A., Polidori, G. and Spagna, R. (2012) *SIR2011*: a new package for crystal structure determination and refinement. *Journal of Applied Crystallography*, **45**, 357–361.

Chenoweth, W.L. (1993) The Geology and Production History of the Uranium Deposits in the White Canyon sMining District, San Juan County, Utah. *Utah Geological Survey Miscellaneous Publication*, **93–3**.

Ferraris, G. and Ivaldi, G. (1988) Bond valence vs. bond length in O···O hydrogen bonds. *Acta Crystallographica*, **B44**, 341–344.

Higashi, T. (2001) *ABSCOR*. Rigaku Corporation, Tokyo.

Kampf, A.R., Plášil, J., Čejka, J., Marty, J., Škoda, R. and Lapčák, L. (2017*a*) Alwilkinsite-(Y), a new rare-earth uranyl sulfate mineral from the Blue Lizard mine, San Juan County, Utah, USA. *Mineralogical Magazine*, **81**, 895–907.

Kampf, A.R., Plášil, J., Kasatkin, A.V., Marty, J. and Čejka, J. (2017*b*) Klaprothite, péligotite and ottohahnite, three new sodium uranyl sulfate minerals with bidentate UO_7–SO_4 linkages from the Blue Lizard mine, San Juan County, Utah, USA. *Mineralogical Magazine*, **81**, 753–780.

Krivovichev, S.V. (2012) Derivation of bond-valence parameters for some cation-oxygen pairs on the basis of empirical relationships between r_o and *b*. *Zeitschrift für Kristallographie*, **227**, 575–579.

Mandarino, J.A. (2007) The Gladstone–Dale compatibility of minerals and its use in selecting mineral species for further study. *The Canadian Mineralogist*, **45**, 1307–1324.

Perles, J., Fortes-Revilla, C., Enrique Gutiérrez-Puebla, E., Iglesias, M., Monge, M.Á., Ruiz-Valero, C. and Snejko, N. (2005) Synthesis, structure, and catalytic properties of rare-earth ternary sulfates. *Chemistry of Materials*, **17**, 2701–2706.

Plášil, J., Kampf, A.R., Kasatkin, A.V. and Marty, J. (2014) Bluelizardite, $Na_7(UO_2)(SO_4)_4Cl(H_2O)_2$, a new uranyl sulfate mineral from the Blue Lizard mine, San Juan County, Utah, USA. *Journal of Geosciences*, **59**, 145–158.

Pouchou, J.-L. and Pichoir, F. (1991) Quantitative analysis of homogeneous or stratified microvolumes applying the model "PAP." Pp. 31–75 in: *Electron Probe Quantitation* (K.F.J. Heinrich and D.E. Newbury, editors). Plenum Press, New York.

Sheldrick, G.M. (2008) A short history of *SHELX*. *Acta Crystallographica*, **A64**, 112–122.

Wood, R.M. and Palenik, G.J. (1999) Bond valence sums in coordination chemistry. Sodium-oxygen complexes. *Inorganic Chemistry*, **38**, 3926–3930.